^{166}Ho-DOTMP Radiation-Absorbed Dose Estimation for Skeletal Targeted Radiotherapy

Hazel B. Breitz, MD[1]; Richard E. Wendt III, PhD[2]; Michael S. Stabin, PhD[3]; Sui Shen, PhD[4];
William D. Erwin, MS[2]; Joseph G. Rajendran, MD[5]; Janet F. Eary, MD; Lawrence Durack[5];
Ebrahim Delpassand MD[2]; William Martin, MD[3]; and Ruby F. Meredith, MD[4]

[1]NeoRx Corp., Seattle, Washington; [2]University of Texas M.D. Anderson Cancer Center, Houston, Texas; [3]Vanderbilt University, Nashville, Tennessee; [4]University of Alabama Comprehensive Cancer Center, Birmingham, Alabama; and [5]University of Washington, Seattle, Washington

^{166}Ho-1,4,7,10-tetraazacyclododecane-1,4,7,10-tetramethylene-phosphonate (DOTMP) is a tetraphosphonate molecule radiolabeled with ^{166}Ho that localizes to bone surfaces. This study evaluated pharmacokinetics and radiation-absorbed dose to all organs from this β-emitting radiopharmaceutical. **Methods:** After two 1.1-GBq administrations of ^{166}Ho-DOTMP, data from whole-body counting using a γ-camera or uptake probe were assessed for reproducibility of whole-body retention in 12 patients with multiple myeloma. The radiation-absorbed dose to normal organs was estimated using MIRD methodology, applying residence times and S values for ^{166}Ho. Marrow dose was estimated from measured activity retained after 18 h. The activity to deliver a therapeutic dose of 25 Gy to the marrow was determined. Methods based on region-of-interest (ROI) and whole-body clearance were evaluated to estimate kidney activity, because the radiotracer is rapidly excreted in the urine. The dose to the surface of the bladder wall was estimated using a dynamic bladder model. **Results:** In clinical practice, γ-camera methods were more reliable than uptake probe–based methods for whole-body counting. The intrapatient variability of dose calculations was less than 10% between the 2 tracer studies. Skeletal uptake of ^{166}Ho-DOTMP varied from 19% to 39% (mean, 28%). The activity of ^{166}Ho prescribed for therapy ranged from 38 to 67 GBq (1,030–1,810 mCi). After high-dose therapy, the estimates of absorbed dose to the kidney varied from 1.6 to 4 Gy using the whole-body clearance–based method and from 8.3 to 17.3 Gy using the ROI-based method. Bladder dose ranged from 10 to 20 Gy, bone surface dose ranged from 39 to 57 Gy, and doses to other organs were less than 2 Gy for all patients. Repetitive administration had no impact on tracer biodistribution, pharmacokinetics, or organ dose. **Conclusion:** Pharmacokinetics analysis validated γ-camera whole-body counting of ^{166}Ho as an appropriate approach to assess clearance and to estimate radiation-absorbed dose to normal organs except the kidneys. Quantitative γ-camera imaging is difficult and requires scatter subtraction because of the multiple energy emissions of ^{166}Ho. Kidney dose estimates were approximately 5-fold higher when the ROI-based method was used rather than the clearance-based model, and neither appeared reliable. In future clinical trials with ^{166}Ho-DOTMP, we recommend that dose estimation based on the methods described here be used for all organs except the kidneys. Assumptions for the kidney dose require further evaluation.

Key Words: ^{166}Ho-DOTMP; skeletal targeted radiotherapy; radiotherapeutic; dosimetry

J Nucl Med 2006; 47:534–542

Multiple myeloma is a malignant disease arising from plasma cells in the bone marrow, with bony involvement leading to cortical bone destruction. The malignancy is both radiosensitive and chemosensitive, with improved response rates, but not cure, reported after myeloablative doses of chemotherapy (1). The addition of skeletal targeted radiotherapy to the conditioning regimen for patients undergoing high-dose chemotherapy and peripheral blood stem cell transplantation has further improved the response rate in phase I and II trials, with promising long-term survival data (2).

^{166}Ho-1,4,7,10-tetraazacyclododecane-1,4,7,10-tetramethylene-phosphonate (DOTMP) is a bone-seeking radiopharmaceutical that has been shown by autoradiography to localize on bone surfaces and may play a role in the management of malignant disease localized in the bone or bone marrow. Radiation is delivered to the skeleton while sparing extraskeletal normal tissue. Thus, the therapeutic index is much improved over that of conventional total-body irradiation.

^{166}Ho is primarily a β-emitter (E$_{max}$, 1.85 MeV) with a maximum pathlength of 8.7 mm in soft tissue and 3.8 mm in bone (derived from standard range/energy tables). ^{166}Ho has a complex energy spectrum for quantitative imaging. A low abundance (7%) of 81-keV photons can be counted and used for γ-camera imaging. There is also a small component (~1%) of high-energy γ-radiation (1.4 MeV) that causes degradation of the images because of septal penetration of the collimator, and approximately 10% x-rays are emitted from 48 to 55 keV. The physical half-life, 27 h, is short enough to permit delivery of high-dose chemotherapy and reinfusion of cryopreserved peripheral blood stem cells

within 6−10 d. This short time frame after myeloablative chemotherapy is advantageous, compared with high-dose ^{131}I or ^{90}Y therapy.

Development of radiopharmaceuticals requires assessment of radiation-absorbed dose. It is therefore important that the methods to acquire adequate data be reproducible and correct at all institutions. A phase I clinical study in patients with multiple myeloma with [166]Ho-DOTMP revealed a high variability in skeletal uptake (3). Patient-specific marrow dose estimates were recommended to calculate the therapeutic activity that will deliver the target radiation-absorbed dose to the marrow (2–4). The methods reported here to estimate radiation-absorbed dose to normal organs for [166]Ho-DOTMP have been updated since the initial reports (3,4).

The objective of this study was to determine the most reliable type of whole-body counting equipment for assessing whole-body retention. Many physicians prefer using a thyroid uptake probe, because this is less time-consuming than a γ-camera scan. The study also evaluated the reproducibility of biodistribution by comparing pharmacokinetics and dosimetric estimates after a second tracer dose of [166]Ho-DOTMP administered 1 wk later and serum pharmacokinetics after the higher therapy dose. The tracer study was used to predict absorbed dose from the therapeutic administration. In the prior trials, kidney dose was estimated using remainder-of-body activity (4,5) and then using the pharmacokinetics model given by the International Commission on Radiological Protection (ICRP) (6,7). Different input data for estimating residence time for the kidney dose were evaluated here because low dose estimates from the prior studies (4) did not predict observed kidney toxicity (2).

This report describes the challenges in quantifying [166]Ho activity with a γ-camera, recommends updated methods for deriving residence times, and provides radiation dose estimates to normal organs from [166]Ho-DOTMP.

MATERIALS AND METHODS

Study Design

This was a multicenter study of skeletal targeted radiotherapy with [166]Ho-DOTMP in 12 patients from 4 institutions. Patients received 2 administrations of 1.1 GBq (30 mCi) of [166]Ho-DOTMP 1 wk apart. Whole-body counting was used to estimate skeletal uptake, to assess clearance of the tracer, and to estimate radiation dose to organs. γ-Camera information from the first tracer study of [166]Ho-DOTMP was used to determine eligibility for therapy and the therapeutic activity required to deliver a 25-Gy dose to marrow. Whole-body retention was also assessed by uptake probe after each tracer administration; thus, 4 whole-body counts for each patient were compared.

All patients underwent continuous bladder irrigation overnight after therapy to prevent hemorrhagic cystitis. This late radiation toxicity was previously observed in several patients who did not receive bladder irrigation after high-dose therapy (2). Serum pharmacokinetics and a single whole-body image were acquired after the therapeutic administration. Patients received a 200 mg/m² dose of melphalan 5−9 d after [166]Ho-DOTMP, followed 24−48 h later by peripheral blood stem cells.

Eligibility Criteria

Patients 18–70 y old who had multiple myeloma and were receiving high-dose chemotherapy and peripheral blood stem cell transplantation were eligible for the trial. The baseline level of creatinine was to be less than 1.8 mg/dL, and baseline creatinine clearance was to be at least 45 mL/min/1.73 m². Absence of kidney obstruction was confirmed by ultrasound. The study was approved by the U.S. Food and Drug Administration and by the institutional review board for each institution, and all patients gave written informed consent.

[166]HO-DOTMP

The [166]Ho was supplied by the University of Missouri Research Reactor as [166]HoCl₃. DOTMP is produced by the phosphonomethylation of 1,4,7,10-tetraazacyclododecane and was supplied by Dow Chemical Co. The HoCl₃ was reacted with DOTMP ligand in a molar ratio of 1:3.5 at a basic pH of 10.5. The resulting [166]Ho-DOTMP chelate was adjusted to a pH of 7 or 8 using phosphate buffer and stabilized with ascorbic acid. The product was then sterile filtered. DOTMP was selected as the ligand to target the [166]Ho to bone because of the high stability of the metal–chelate complex.

Data Acquisition for Dosimetry

Whole-body counts were obtained at 7 time points (nominally 0.5, 4, 20, 24, 28, 44, and 48 h) after administration of each tracer dose using a γ-camera and an uptake probe. A system calibration standard with a known amount of [166]Ho, ~3.7 MBq in 200 mL of water, was counted to correct for any observed system variability.

γ-Camera Counting. A medium-energy collimator was used with a 20% energy window over the 81-keV photopeak. This collimator was chosen as a compromise between scatter reduction and sensitivity for the quantification. The studies were done on Hawkeye (GE Healthcare), ECAM (Siemens), and Axis (Philips) systems. The crystal thicknesses of the cameras varied: 3/8, 5/8, and 6/8 in. (0.9525, 1.5875, and 1.9050 cm, respectively). The cameras were set for a 10-min scan at the first time point and then for a longer duration, up to 30 min, for subsequent scans. Counts from a region of interest (ROI) over the whole body, the standard, and nearby background were recorded at each time point. Initially, the standard was positioned between the patient's feet and was counted with the patient. The counts in the standard ROI did not decrease at the physical half-life of [166]Ho, probably because bladder counts were scattering into the standard ROI; thus, this approach was revised and the calibration standard was then scanned separately at each time point. Images were evaluated to confirm that no radioactivity was present outside the skeleton, except for the kidneys and bladder.

Probe Counting. Anterior and posterior 1- or 2-min counts from the patient, the standard, and room background were obtained with an uptake probe using an energy window of 60–100 keV. The patient and standard were positioned in a reproducible geometry 3 m from the probe.

Pharmacokinetics Analysis. Plasma samples were obtained at 5, 30, and 50 min and at 1, 2, 3, 4, 6, 20, and 24 h after infusion of both tracers and the therapy administration. Urine volume was measured, and aliquots were counted from collections obtained at 1, 2, 3, 4, 6, 12, 24, and 44 h. Cumulative urine activity from the tracer studies was compared with whole-body counts to confirm that whole-body

counting was a valid method to assess urinary excretion for radiation-absorbed dose estimates. Plasma ^{166}Ho-DOTMP concentration–time data were analyzed by a 2-compartment method, using WinNonlin Enterprise software, version 3.2 (Pharsight).

Kidneys. The transit time through the kidneys for the ICRP model (*6*) was estimated from a dynamic kidney scan, and data were analyzed by a compartment model using SAAM software (SAAM Institute, Inc.) (*8*) to derive the time to peak activity. A γ-camera–based method for estimating kidney dose was evaluated during this trial. Images were acquired for triple-energy-window scatter correction (*9,10*). A 20% window over the 81-keV photopeak (16 keV) and a window of equal width immediately above this window were set in order to subtract counts from Compton-scattered photons from septal penetration of the 1.4-MeV photons in the patient, collimator, and crystal. The third window was a narrower window (10 keV) just below the 81-keV photopeak, between it and the x-ray peaks, to subtract Compton scatter from within the photopeak window. Data were obtained from 5-min images of the kidneys at 6 time points within 20 h. Phantom studies at each site had provided counts from ^{166}Ho at different depths through acrylic sheets, and these were used to estimate the effective attenuation coefficient, μ (cm^{-1}), for ^{166}Ho specific for each camera system. With the medium-energy collimator, the effective attenuation coefficient for ^{166}Ho was 0.131 or 0.158 cm^{-1}, depending on the imaging system. Kidney ultrasound was performed to measure the depth of the kidneys, and 3 kidney dimensions were measured to estimate mass (*11*).

Radiation-Absorbed Dose Estimates

Radiation-absorbed dose was estimated using the MIRD methodology (*5*), and residence times were derived. Tables of S values for ^{166}Ho were obtained from Oak Ridge Associated Universities (*12,13*). These values had been calculated using the same assumptions as those in the MIRDOSE3 code (*14*).

Marrow Dose. Serial imaging showed that by 18 h after injection, the radioactivity remaining in the whole body was localized mostly in the skeleton. Therefore, the skeletal residence time could be determined using a monoexponential fit for the last 5 time points (from 18 h onward). The trabecular bone surface of the skeleton is the primary source of radiation to the marrow because of its close proximity, whereas the contribution from cortical bone and other source organs is negligible (*14*). Distinguishing the proportion of these 2 types of bone and their relative surface area is important for the dose calculations. The published ratio of trabecular to cortical bone surface area is 62:38 (*15*).Thus, for marrow dose estimates from the trabecular bone surface, the residence time becomes 0.62 times the skeletal residence time. The marrow mass, and thus the S value for the marrow dose, was adjusted according to the patient's body surface area (*16*), using a ratio of 1.8:patient body surface area (1.8 m^2 is the body surface area for reference man) (*14*). The total dose to marrow was the sum of the products of residence times and S values to marrow for the trabecular bone, cortical bone, kidney, bladder, and remainder of body.

Whole- and Remainder-of-Body Residence Times. The fraction of injected activity remaining in the patient was derived from the geometric means of the anterior and posterior whole-body counts at each of the 6 time points normalized by that of the first, immediate, measurement. This whole-body time–activity curve was used to derive a whole-body residence time by fitting a 2-component exponential function to the whole-body time–activity curve and integrating the resultant function from zero to infinity.

The remainder-of-body residence time was derived by subtracting the residence times of the skeleton, bladder, and kidney from the whole-body residence time.

Urinary Tract. The disappearance of radioactivity from the whole body was used to estimate the exposure to the urinary tract based on the results.

Kidneys. The kidney residence time for the ICRP model (*6*) was derived from the sum of the residence time in urine and blood components. Whole-body counting gave an assessment of the amount of activity and the rate of excretion through the kidneys. The transit time was estimated from the dynamic kidney scan. These data gave the residence time from urine in the kidneys. The residence time for radioactivity in the blood was determined from pharmacokinetics analysis, using a 2-compartment exponential fitting of the blood time–activity curve scaled by 0.02 because the kidneys contain ~2% of the blood volume (*17*). For the γ-camera ROI-based kidney dose, kidney ROIs were drawn over posterior images with nearby background subtraction. In most cases, the kidneys could not be visualized on the anterior images beyond 3 h (Fig. 1). Each time the patient was imaged, the counts from the calibration standard and a background ROI next to the standard were recorded from the 3 windows. Photopeak window counts were corrected for scatter by subtracting the average of both scatter window counts normalized for each kilovoltage window width (*9,10*). The net kidney counts were then corrected for attenuation using the effective attenuation based on the depth of the kidneys. The residence time was derived from trapezoidal integration of the time–activity data out to 20 h; beyond 20 h, the residence time was derived from the slope of the curve between 6 and 20 h.

The residence time calculated for each method (ICRP and ROI-based) was multiplied by the S value for the adult kidney adjusted for the mass of the kidneys, derived from the ultrasound measurements (*11*).

Bladder. The dose to the bladder surface from activity in the bladder contents was estimated using the revised MIRD dynamic bladder model MIRD 14 (*18*) modified to represent a catheterized, irrigated bladder.

Estimation of Absorbed Dose for Other Normal Organs. Remainder-of-body S values were derived according to the standard
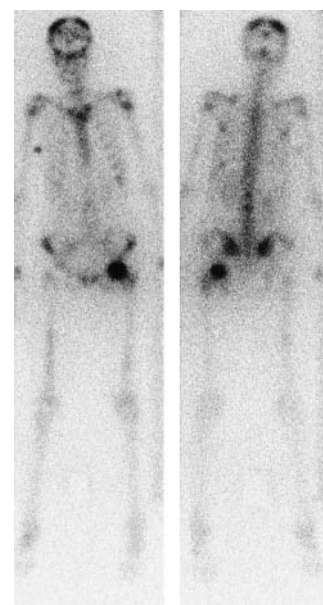
FIGURE 1. Anterior (right) and posterior (left) whole-body images 18 h after administration of 1.1 GBq of ^{166}Ho-DOTMP.

MIRD method (5). The whole-body and kidney S values were adjusted for actual mass from each patient. Other organ masses were based on reference adult organ masses. The S values for the reference adult model were used because all patients weighed more than 63 kg.

Assessing Eligibility for High-Dose Therapy

The skeletal residence time was represented by $Y = F \times T_e$, where F represents the estimate of initial uptake of ^{166}Ho-DOTMP in the skeleton and T_e the effective half-time of the radioactivity in the skeleton calculated from the slope of the natural log of the curve, λ ($T_e = \ln2/\lambda$). These skeletal uptake and retention data obtained from the γ-camera after the first administration of tracer were used to confirm eligibility for continuation in the study and to derive the therapeutic dose from the marrow dose estimate. The criterion to receive therapy was a skeletal residence time of 5.8 h ($F \times 1.44 \times T_e$) based empirically on an initial skeletal uptake, an F of at least 16% of the injected activity, and an adequate retention in the skeleton. The correlation coefficient for the time–activity curve fit was used as a measure of reliability of the data; an r^2 value of at least 0.97 was selected as the lower-level cutoff of acceptability. F, T_e, and the therapeutic dose were determined from both camera and probe for each of the 2 tracer administrations. All 4 evaluations provided information on intrapatient reproducibility from calculations of therapeutic dose. The comparisons of γ-camera and probe whole-body counting provided information on whether the two would result in the same prescribed activity for therapy and thus could be interchangeable.

The activity to be administered for therapy was derived by dividing the required dose, 25 Gy, by the absorbed dose from the trabecular bone component per unit administered activity, as derived from the γ-camera data.

RESULTS

Twelve patients (6 men and 6 women) aged 48–67 y with multiple myeloma were studied with 2 tracer administrations followed by a therapeutic administration of 38–67 GBq to deliver 25 Gy to marrow.

Imaging

Localization in the skeleton was observed by the second imaging time point, 4−6 h. Bladder activity was prominent immediately after injection and was still visible at 4−6 h, associated with rapid excretion of the nontargeted radiopharmaceutical, but was not observed at later times. The kidney activity was variable but never persistent. In some patients, posterior kidneys were visible only till 2−3 h, but in general they were visible till 4−6 h and barely perceptible from 20 h onward. No other normal tissue was visualized (Fig. 1).

^{166}Ho Spectra

Figure 2A shows the spectrum from ^{166}Ho obtained on an ECAM γ-camera with a 3/8-in. (0.9525 cm) crystal and no collimator. The primary photopeak at 81 keV is apparent, as are the x-ray peaks from 48 to 55 keV. Above the 81-keV peak, relatively few counts are detected because the crystal is largely transparent to the high-energy photons. The spectrum in Figure 2B was measured through a medium-
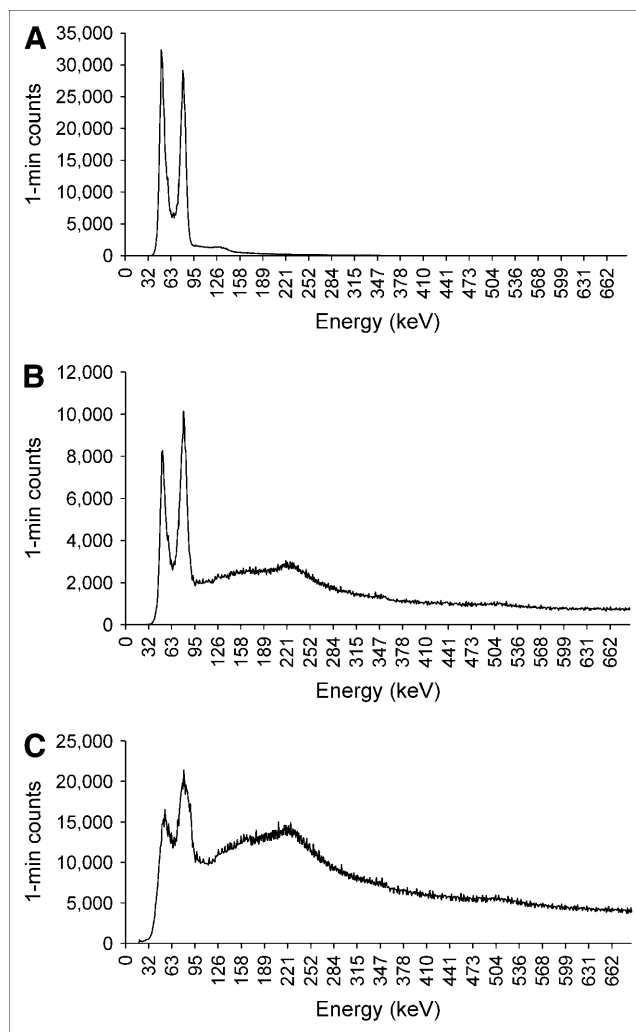
FIGURE 2. (A) ^{166}Ho energy spectrum on γ-camera from point source without collimator. (B) ^{166}Ho energy spectrum on camera with medium-energy collimator. (C) For a patient, ^{166}Ho energy spectrum on camera with medium-energy collimator.

energy collimator. The collimator attenuates the lower-energy photon flux, making the higher-energy γ-rays that are not attenuated by the collimator far more prominent. Figure 2C is from ^{166}Ho in a patient. The additional counts in the spectrum represent Compton-scatter high-energy photons in both patient and crystal, including those that have penetrated the collimator septa, resulting in the production of lower-energy photons and the addition of lead x-rays under the 81-keV photopeak (19) and Compton scatter from the 81-keV photons. Triple-energy-window scatter subtraction (9,10) was applied to remove these contributions so that the counts measured would be more representative of the 81-keV counts for the ROI-based method of kidney dose estimation.

Assessment of Whole-Body Counting Methods

Table 1 summarizes the skeletal uptake and clearance parameters F and T_e and the residence time from the

TABLE 1
Skeletal Parameters from γ-Camera Data

Parameter	F	T_e (h)	Residence time	r^2	Activity calculated to deliver 25 Gy of ^{166}Ho-DOTMP to marrow GBq (mCi)	GBq/m²(mCi/m²)
Median	0.28	22.4	8.67	0.993	49.09 (1,326)	25.7 (695)
Minimum	0.19	18.5	6.70	0.980	38.15 (1,030)	19.5 (528)
Maximum	0.39	24.9	11.4	1.000	67.04 (1,810)	33.3 (899)

F = estimated fraction of injected activity in skeleton at time 0; T_e = effective half-life; r^2 = correlation coefficient from curve fit of time–activity data.

γ-camera after the first tracer dose. γ-Camera data from the 2 tracer administrations demonstrated that both F and T_e varied among patients but were consistent within patients. The average absolute percentage differences in F and T_e within patients were 10% and 8%, respectively. The largest difference between marrow dose calculated from tracer administration 1 and tracer administration 2 was 15%. Paired t test results were not significant ($P > 0.05$). The data were considered reliable in all patients ($r^2 \geq 0.97$ for all studies), supporting use of a tracer administration to determine the therapeutic dosage and to estimate radiation-absorbed dose after the therapeutic administration.

Uptake probe data showed the average absolute percentage changes in F and T_e within patients to be 28% and 7%, respectively. Dose estimates based on probe counting differed by 25%, on average, between the 2 administrations,

with a median absolute percentage difference of 13%. Estimates of therapeutic activity from the probe were 2 or more times more variable than those from the γ-camera. In 5 of the 12 studies, the criterion for curve fit of data was not met with probe counting.

Radiation-Absorbed Dose

Table 2 shows the median dose to all organs, as mGy/MBq and cGy/mCi, and the median radiation-absorbed dose estimates from the activity that was actually injected for therapy. Following high-dose therapy, the bladder dose ranged from 10 to 20 Gy, bone surface dose ranged from 39 to 57 Gy, and dose to other organs was less than 2 Gy for all patients. A comparison was made with marrow dose estimates based on 3 late time points, excluding the 28- and 48-h time points. The fewer data points were equally accurate for these

TABLE 2
Doses to MIRDOSE Target Organs

Target organ	Median mGy/MBq	Median rad/mCi	SD mGy/MBq	SD rad/mCi	Median from therapy (cGy)
Adrenals	0.014	0.050	0.0054	0.020	64
Brain	0.014	0.051	0.0054	0.020	64
Breasts	0.013	0.048	0.0054	0.020	61
Gallbladder wall	0.013	0.049	0.0054	0.020	62
Lower large intestine wall	0.014	0.050	0.0054	0.020	63
Small intestine	0.013	0.049	0.0054	0.020	62
Stomach	0.013	0.049	0.0054	0.020	62
Upper large intestine wall	0.013	0.049	0.0054	0.020	62
Heart wall	0.013	0.049	0.0054	0.020	62
Kidneys	0.045	0.167	0.0121	0.045	210
Liver	0.013	0.049	0.0054	0.020	62
Lungs	0.014	0.050	0.0054	0.020	63
Muscle	0.013	0.049	0.0054	0.020	63
Testes	0.013	0.049	0.0054	0.020	62
Pancreas	0.013	0.049	0.0054	0.020	63
Red marrow	0.517	1.913	0.0820	0.304	2,400
Bone surfaces	0.920	3.404	0.1650	0.612	4,300
Skin	0.013	0.049	0.0054	0.020	62
Spleen	0.013	0.049	0.0054	0.020	62
Thymus	0.013	0.049	0.0054	0.020	62
Thyroid	0.014	0.050	0.0054	0.020	63
Urinary bladder wall	0.291	1.078	0.0150	0.054	1,400
Uterus	0.013	0.049	0.0054	0.020	62
Total body	0.062	0.229	0.0057	0.021	290

purposes. The average difference between 3- and 5-data-point dose estimates for the 12 patients was 0.23% ± 0.01%.

Kidney Dose Using ICRP Model. The time to peak activity in the kidney ranged from 0.87 to 2.35 min in 12 kidneys (6 patients). For all patients, 3 min was used as a conservative estimate of transit time. The average dose was 0.048 mGy/MBq and was consistent between administrations (Table 3), and the total kidney absorbed dose estimate varied from 1.6 to 4 Gy. The blood activity contributed less than 1% of the dose to the kidneys. The majority of the activity (mean, 83%; range, 61%−98%) was excreted in the first 12 h. The dose rate to the kidneys peaked immediately after injection at an estimated 70 cGy/h and then decreased rapidly. The linear quadratic approach was used to estimate the biologically effective dose (20,21). As a result of the initially high dose rate, assuming a 1-h repair time for kidney tissue and an α/β-ratio of 2.4 and including a constant for incomplete repair (7,20), the relative effectiveness for the kidneys was 1.3 and the calculated biologically effective dose may therefore have been 30% higher than the doses estimated.

Kidney Dose Using ROI Methodology. In general, estimates from the ROI-based data suggest an approximately 0.27 mGy/MBq kidney dose of ^{166}Ho-DOTMP (Table 3), with the total estimated dose being 8.3–17.3 Gy. About 90% of total counts were subtracted using background subtraction and triple-energy-window scatter subtraction for ^{166}Ho-DOTMP (Fig. 3). Evaluation of the adjusted count data appeared unreliable for accurate dose estimates for individual patients, because time–activity curves frequently did not conform to those expected from biologic data. Although images and unsubtracted, raw count data from the kidney ROI of the same patient twice consistently suggested reproducible behavior of the ^{166}Ho-DOTMP in both kidneys, this suggestion was not consistent with the variability seen in the doses estimated using these ROI data (Table 3). Difficulties were encountered in quantifying counts from poor statistics from the low-energy, low-abundance photopeak and the complex effects of scatter and septal penetration of the high-energy photon on the γ-camera that may not be accurately corrected by the applied triple-energy-window subtraction method. Figure 3 shows a plot of uncorrected counts from a patient from the 81-keV window within the ROI for each kidney versus time and the same kidney data after background and scatter subtraction.

The findings for certain patients are mentioned in the footnotes of Table 3. In 6 kidneys, either data were not used at all or the half-life was limited by the physical half-life of the radioisotope for the calculations. For 9 patients, the doses varied by up to 30% from one week to the next, but the variations were much greater in 2 patients, 51% and 97%. This variability was greater than that observed using whole-body counting and pharmacokinetics data, which were relatively reproducible between administrations.

Pharmacokinetics

Plasma Pharmacokinetics. The observed peak concentration from individual patients was similar (7.93% ± 2.82% injected activity/L). The mean half-lives for the α- and β-phases were 0.72 ± 5.6 and 6.16 ± 7.68 h, respectively. The mean residence time was 4.6 ± 3.82 h. The initial decline in concentration represents a combination of tissue distribution and drug elimination. The mean central and steady-state volumes of distribution were 14.6 ± 8.1

TABLE 3
Kidney Dose Estimates

Patient no.	γ-Camera dose estimate (mGy/MBq)		Pharmacokinetics model dose estimate (mGy/MBq)	
	Administration 1	Administration 2	Administration 1	Administration 2
02	0.299	ND	0.069	0.073
03	0.277	0.337*	0.049	0.122
04	0.207	0.154	0.036	0.034
05	0.259*	0.208	0.041	0.041
06	0.277	0.462*	0.053	0.057
07	0.291	0.216	0.054	0.056
08	0.216	0.199	0.039	0.040
09	0.221	0.154	0.058	0.059
10	ND	0.232	0.041	0.041
11	0.296	0.585	0.036	0.038
12	0.237	0.286*	0.031	0.031
14	0.294†	0.315	0.072	0.064
Average	0.261	0.283	0.048	0.048
SD	0.027	0.018	0.012	0.014

*Late residence time used physical decay because, inconsistent with imaging and physical half-life, scatter-corrected data showed increasing counts beyond 4 h.

†Negative counts in photopeak after scatter subtraction in 1 kidney.

ND = no data available, technical problems with camera.

In several of these patients, data from only 1 kidney were used for kidney dose estimates.
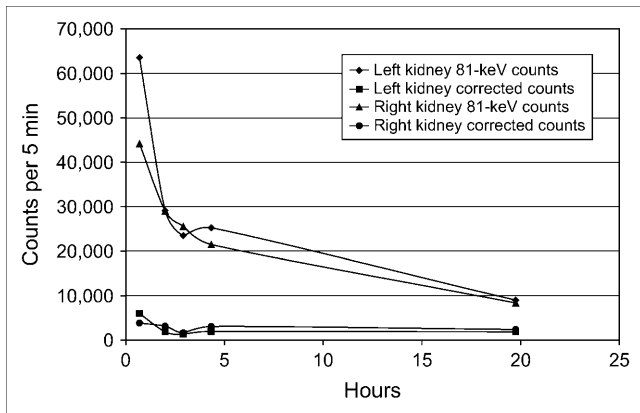
FIGURE 3. For patient 12, kidney ROI counts from 81-keV window before and after correction for background and scatter.

and 34.5 ± 27.8 L, respectively, indicating a relatively restricted distribution of ^{166}Ho-DOTMP into vascular and extravascular body water. Mean systemic clearance was 7.06 ± 1.67 L/h.

Urine Pharmacokinetics. The majority of the drug was recovered in the urine. Cumulative excretion for 12 patients is shown in Figure 4. By the first void, at less than 1.3 h, 26% ± 12% had been excreted.

Renal Clearance. Renal clearance was estimated from plasma and urine data and was similar for all patients, 6.09 ± 1.71 L/h. (102 mL/min). This is similar to the mean baseline creatinine clearance in this study population, 75 mL/min.

The fraction remaining in whole body was compared with cumulative urinary excretion. The sum of the whole-body activity from counts retained, either by camera or uptake probe, and the amount excreted in the urine, was close to 100% of the total injected activity. In general, the added urine and whole-body data were slightly higher than the total dose injected, all within 108%. All radioactivity
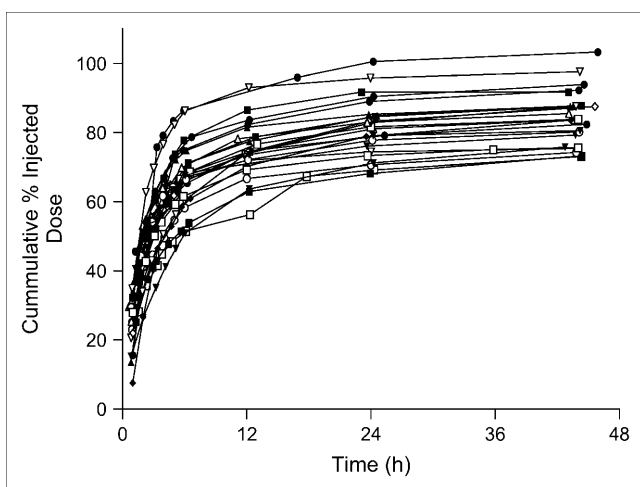
FIGURE 4. Cumulative excretion of tracer in aliquots of urine collected from each patient after each tracer dose. Errors in measuring urine volume may have accounted for high cumulative excretion in some patients.

not bound to skeletal tissue was rapidly excreted in the urine, with no binding evident in other normal organs. This assessment was based on pharmacokinetics analysis and serial imaging over 48 h. All excretion had occurred by 24 h.

DISCUSSION

The estimates of radiation-absorbed dose were based on MIRD principles, using residence times determined from quantitative γ-camera imaging combined with specific absorbed fractions from tables of S factors. Several lessons learned in this study are relevant for dosimetry from radiophosphonates as regards whole-body counting, kidney dosimetry, and marrow dose.

The 2 counting systems—the whole-body γ-camera scan and the probe—are not equivalent for 1.1 GBq of ^{166}Ho. The data were acquired within minutes of each other, with no urinary voiding in between, so the difference in the calculated ^{166}Ho-DOTMP activities to deliver a target bone marrow dose are most likely due to technical differences. For 8 of 12 patients (67%), the residence time was higher when a γ-camera was used. The probe was considered less reliable because of the nonreproducibility of patient positioning and the poorer quality control at the clinical sites. Therefore, in general, the γ-camera was more reproducible within patients from week to week, and the data were more consistent as reflected by the r^2 values from the late whole-body curves. For future assessments of skeletal uptake, whole-body counts obtained with a γ-camera would be preferable.

Based on the result that no appreciable difference existed between the marrow dose estimates with 3 and with 5 of the later time points for activity that clears monoexponentially and mostly by physical decay, the use of more than 3 time points over a 30-h period is not necessary.

The assumptions used for estimating marrow dose from ^{166}Ho-DOTMP have been modified since studies using other radiophosphonate molecules were first reported (*22–25*). In those studies, the radioactivity was assumed to be localized initially in the entire bone and then on the bone surface, and equal distribution on trabecular and cortical bone was assumed (*26*). Updated values of the relative surface areas of trabecular and cortical bone (*4,7,15*) account for a 20% higher dose estimate than previously reported. Small molecules such as phosphonates and peptides leave the intravascular compartment so rapidly that the whole-body or remainder-of-body activity is considered a secondary contributor after the bone itself. In this study, this contribution accounted for less than 2% of the dose to the marrow. The contribution from the cortical bone component was negligible.

Both blood and urine pharmacokinetics demonstrated consistent and reproducible behavior for ^{166}Ho-DOTMP, and the plasma pharmacokinetics of the tracer administration were representative of the therapeutic administration. With use of the γ-camera, the activity calculated to deliver 25 Gy to the marrow was reproducible within patients, with

an average percentage difference of less than 10% between tracer studies. This finding suggests that DOTMP binding sites are not saturated after the first tracer administration and therefore implies that tracer administration does not affect uptake of the therapeutic administration.

Difficulties in precisely estimating urine volumes may explain the small differences between activity injected and the sum of the percentage of activity remaining in skeleton and the amount excreted in urine. These results confirm that estimates of bone uptake from whole-body counting are comparable to those obtained from urinary excretion data; thus, the whole-body counting was validated by the pharmacokinetics analysis.

The calculated therapeutic activity needed to deliver the target bone marrow dose ranged widely as a function of differences in skeletal uptake and clearance among patients, as well as differences in body surface area. Based on the γ-camera data, this range was 38–67 GBq (1,030–1,810 mCi).

Whole-body imaging and ROI counts over the kidneys indicated a rapid decrease in activity from the kidneys, consistent with the pharmacokinetics analysis. This decrease suggested that the unbound plasma clearance of ^{166}Ho-DOTMP is similar to that of creatinine, consistent with passive renal filtration of unbound ^{166}Ho-DOTMP from the plasma, with minimal tubular reabsorption or secretion, and that the ICRP model should be a valid approach for dosimetry estimation The γ-camera method was found to be unreliable because of the complex spectrum of ^{166}Ho and the difficulty of quantifying ^{166}Ho activity with a γ-camera. γ-Camera–based methodology has been used for other γ-emitting radionuclides, but those studied up till now have not had a spectrum contaminated by photons with as high an energy as the 1.38-MeV photons of ^{166}Ho. Where there is a low target-to-background count ratio, accuracy in measuring activity is reduced. With the low yield of the 81-keV photons (7%), and the rapid excretion of ^{166}Ho-DOTMP via the kidneys, the background-subtracted counts in the ROI are quite low at 18 h, thus greatly increasing the noise because of poor statistics. In these studies where kidney activity was barely above the background activity for most of the data points, it was difficult to obtain a reasonable assessment of activity. Errors appear to have arisen as the data were adjusted for scatter and background. Further work on scatter subtraction techniques is required.

The transit time of radioisotope through the kidney used for the ICRP model was assumed to be the same as the time to peak activity in the kidneys. Although this measurement may not precisely represent the mean transit time in the kidney, it provides an approximation that can be used in this model for kidney dose estimation. The rapid time to peak can be explained by the aggressive hydration. The question of why, in the prior dose escalation phase I and II trials using the same assumptions and methodology, radiation nephropathy occurred at doses far lower than the threshold for injury predicted by external-beam criteria was not answered (*4,7*). In those trials, renal toxicity occurred when the dose was above 400 cGy (*17*). Administered activity less than 27.8 GBq/m^2 (750 mCi/m^2) or not exceeding 55.5 GBq (1,500 mCi) was found to be safe, based on retrospective analysis of those trials, following patients for more than 4 y. No grade 4 kidney toxicity was observed at activity levels less than 55.5 MBq, and only 1 case of grade 3 toxicity was observed, in a patient with progressive multiple myeloma (*27*). There have been no cases of grade 3 or 4 kidney or bladder toxicity in the 12 patients treated in the study described in this report, for whom at least 34 mo have now passed after therapy.

In patients with multiple myeloma, CT of the kidneys is avoided because of possible contrast medium reactions. Thus, ultrasound measurements were used to assess kidney mass and depth for attenuation correction. This, however, was another factor that introduced variability into the dosimetry. γ-Camera images are acquired with the patients lying on their back. With ultrasound, the depth often can be measured only when patients are on their side or prone, and the extent to which the kidneys move when patients change position is not known. Therefore, the depth recorded by ultrasound may not be the same as that for γ-camera imaging. Theoretically, a difference in depth of 1 cm would change the attenuation correction factor by 16%. For example, the uncorrected data from patient 11 showed similar counts for both kidneys. However, the depth of one kidney was measured to be 3.3 cm deeper than the other, resulting in a 1.7-fold difference in the attenuation factor between the 2 kidneys and, therefore, in the counts used for the dose calculation.

CONCLUSION

Twelve patients with multiple myeloma at 4 institutions provided data for 24 dosimetry evaluations from ^{166}Ho-DOTMP. Although the methods used to estimate dosimetry in this trial appear reasonable considering the difficulty of imaging a ^{166}Ho-labeled small molecule, the method used to prescribe the activity for therapy is not necessary. The prescribed therapeutic activity in the phase I and II studies and in this study was based on delivering the maximum tolerated dose to the marrow, because that was believed to be the target organ for radiation damage. The efficacy and late toxicities observed indicated that even at these high activities, the marrow was not the dose-limiting organ; the marrow recovered normally in all patients with peripheral blood stem cell transplantation. The kidneys and bladder were the critical organs. The prescribed dose, based on body surface area, was as reliable as kidney dose in ensuring safety and is more practical for this radiopharmaceutical product.

This study demonstrated that the methodology for marrow dosimetry can be standardized across multiple clinical sites and that data can be acquired consistently when a

γ-camera is used for whole-body counting. In contrast, whole-body counting with an uptake probe was significantly more variable and less reliable. The radiation-absorbed dose methodology described here to estimate dose to all organs other than the kidney is recommended for future studies. An optimal method to establish kidney dose for ^{166}Ho-DOTMP was not defined, and the methods described require further evaluation.

ACKNOWLEDGMENTS

REFERENCES

1. Child AH. High dose chemotherapy with hematopoietic stem-cell rescue for multiple myeloma. *N Engl J Med.* 2003;348:1875–1883.
2. Giralt S, Bensinger W, Goodman M, et al. ^{166}Ho-DOTMP plus melphalan followed by peripheral blood stem cell transplantation in patients with multiple myeloma: results of two phase I/II trials. *Blood.* 2003;102:2684–2691.
3. Bayouth JE, Macey DJ, Kasi LP, et al. Pharmacokinetics, dosimetry and toxicity of holmium-166 DOTMP for bone marrow ablation in multiple myeloma. *J Nucl Med.* 1995;36:730–737.
4. Rajendran J, Eary J, Bensinger W, Durack L, Vernon C, Fritzberg A. High-dose ^{166}Ho-DOTMP in myeloablative treatment of multiple myeloma: pharmacokinetics, biodistribution, and absorbed dose estimation. *J Nucl Med.* 2002;43:1383–1390.
5. Loevinger RL, Budinger TF, Watson EE. *MIRD Primer for Absorbed Dose Calculations.* Reston, VA: Society of Nuclear Medicine; 1999:5–6.
6. International Commission on Radiological Protection. *ICRP Publication 53: Radiation Dose to Patients from Radiopharmaceuticals.* Elmsford, NY: Pergamon Press; 1987:18–19.
7. Breitz HB, Wendt R, Stabin M, Bouchet L, Wessels B. Dosimetry of high dose skeletal targeted radiotherapy (STR) with ^{166}Ho-DOTMP. *Cancer Biother Radiopharm.* 2003;18:225–230.
8. Foster D, Barrett P. Developing and testing integrated multicompartment models to describe a single-input multiple-output study using the SAAM II software system. In: *Proceedings of the Sixth International Radiopharmaceutical Dosimetry Symposium.* Oak Ridge, TN: Oak Ridge Institute for Science and Education; 1999:577–599.
9. Ogawa K, Ichihara T, Kubo A. Accurate scatter correction in single photon emission CT. *Ann Nucl Med Sci.* 1994;7:145–150.
10. Ogawa K, Harata Y, Ichihara T, Kubo A, Hashimoto S. A practical method for position-dependent Compton-scatter correction in single photon emission CT. *IEEE Trans Med Imaging.* 1991;10:408–412.
11. Kasiske BL, Umen AJ. The influence of age, sex, race, and body habitus on kidney weight in humans. *Arch Pathol Lab Med.* 1986;110:55–60.
12. Cristy M, Eckerman KF. *Specific Absorbed Fractions of Energy at Various Ages from Internal Photon Sources.* Oak Ridge, TN: Oak Ridge National Laboratory; 1987. ORNL report ORNL/TM-8381/V1-V7.
13. Eckerman K, Stabin M. Electron absorbed fractions and dose conversion factors for marrow and bone by skeletal regions. *Health Phys.* 2000;78:199–214.
14. Stabin M. MIRDOSE: personal computer software for internal dose assessment in nuclear medicine. *J Nucl Med.* 1996;37:538–546.
15. International Commission on Radiological Protection. *ICRP Publication 70: Basic Anatomical and Physiological Data for Use in Radiological Protection—The Skeleton.* Elmsford, NY: Pergamon Press; 1997:23.
16. Breitz HB. Dosimetry in a myeloablative setting. *Cancer Biother Radiopharm.* 2002;17:119–128.
17. Leggett RW, Williams LR. A proposed blood circulation model for reference man. *Health Phys.* 1995;69:187–201.
18. Thomas SR, Stabin MG, Chen CT, Samaratunga RC. MIRD pamphlet no. 14 revised: a dynamic urinary bladder model for radiation dose calculations. *J Nucl Med.* 1999;40:102S–123S.
19. Erwin WD, Wendt RE III, Breitz HB. Physical simulation of gamma camera imaging of ^{166}Ho [abstract]. *J Nucl Med.* 2003;44(suppl):139P.
20. Dale RG. Dose-rate effects in targeted radiotherapy. *Phys Med Biol.* 1996;41:1871–1884.
21. Dale R. Use of linear-quadratic model for quantifying kidney dose response in targeted radiotherapy. *Cancer Biother Radiopharm.* 2004;19:363–370.
22. Eary JF, Collins C, Stabin M, et al. Samarium-153-EDTMP biodistribution and dosimetry estimation. *J Nucl Med.* 1993;34:1031–1036.
23. Liepe K, Hlisces R, Kropp J, Runge R, Knapp R Jr, Franke W-G. Dosimetry of ^{188}Re-hydroxyethylidene diphosphonate in human prostate cancer skeletal metastases. *J Nucl Med.* 2003;44:953–960.
24. Turner JH, Claringbold PG, Hetherington EL, Sorby P, Martindale AA. A phase I study of samarium-153 ethylenediaminetetramethylene phosphonate therapy for disseminated skeletal metastases. *J Clin Oncol.* 1989;7:1926–1931.
25. Heggie J. Radiation absorbed dose calculations for samarium-153-EDTMP localized to bone. *J Nucl Med.* 1991;32:840–844.
26. International Commission on Radiological Protection. *ICRP Publication 20: Report of the Task Group on Reference Man—Anatomical, Physiological and Metabolic Characteristics.* Oxford, U.K.: Pergamon Press; 1975.
27. Giralt S, Bensinger W, Goodman M, Gray D, Sims R, Breitz HB. Long-term safety and efficacy data supporting new dosing of ^{166}Ho-DOTMP for skeletal targeted radiotherapy for multiple myeloma. *Blood.* 2003;102:2684–2691.